SUPPORTING INFORMATION

Development of tin oxide catalysts promoting the ring-closing depolymerization of poly(ε-caprolactone) under mild conditions

Tetsu Nakatani,[a,b] Kohei Mishima,[a] Sho Yamaguchi,[c] Akira Miura,[d] Takato Mitsudome,*[a,e] and Tomoo Mizugaki**[a,e,f]

[a]Department of Materials Engineering Science, Graduate School of Engineering Science, The University of Osaka, 1-3 Machikaneyama, Toyonaka, Osaka 560-8531, Japan.
[b]Functional Products BU, Smart SBU, Daicel Corporation, 1239 Shinzaike, Aboshi-ku, Himeji, Hyogo 671-1283, Japan.
[c]Department of Chemical Science and Engineering, Kobe University, 1-1 Rokkodai, Nada-ku, Kobe 657-8501, Japan.
[d]Faculty of Engineering, Hokkaido University, Kita 13-jo, Nishi 8-chome, Kita-ku, Sapporo, Hokkaido, 060-8628 Japan.
[e]Innovative Catalysis Science Division, Institute for Open and Transdisciplinary Research Initiatives (ICS-OTRI), The University of Osaka, Suita, Osaka 565-0871, Japan.
[f]Research Center for Solar Energy Chemistry, Graduate School of Engineering Science, Osaka University, 1-3 Machikaneyama, Toyonaka, Osaka 560-8531, Japan.
*Corresponding Author: Email: mitsudom@cheng.es.osaka-u.ac.jp
**Corresponding Author: Email: mizugaki.tomoo.es@osaka-u.ac.jp

Table of Contents

1. General experimental details

All organic and inorganic reagents were used as received. SnO, SnO_2, MgO, poly(ε-caprolactone) (*M*w 10000 g mol^{-1}), polyethylene glycol (*M*w 400 g mol^{-1}), tetrahydrofuran (THF), biphenyl and chloroform-d (d, 99.8%, containing 0.05% (v/v) tetramethyl silane (TMS) and silver foil) were purchased from FUJIFILM Wako Pure Chemical. ZnO was purchased from Nacalai Tesque, Inc. γ-Al_2O_3 was purchased from Strem Chemicals, Inc. TiO_2 (JRC-TIO-16) was supplied by the Catalyst Society of Japan as reference catalysts.

^{1}H nuclear magnetic resonance (NMR) spectra were recorded using a JEOL JNM-ESC400 spectrometer. In-situ synchrotron X-ray diffraction (SXRD) measurements were performed at BLXU13 beamline in the SPring-8, Japan Synchrotron Radiation Research Institute (JASRI), Harima, Japan, with the approvals of 2025A02141.[S1] The samples were sealed in a quartz capillary with a diameter of 0.3 mm. The sealed samples were automatically changed by a robotic system, and heated at 80 °C min^{-1} from 60 to 800 °C. The wavelength was 0.354443 Å. Powder X-ray diffraction (XRD) patterns were acquired using a Philips X′Pert-MPD diffractometer with Cu-Kα radiation (45 kV, 40 mA). Nitrogen adsorption–desorption isotherms were measured at liquid nitrogen temperature and a relative pressure (P/P°) range of 0.001–1 using a BELLSORP-MAX instrument (BEL Japan Inc.). Samples were filled in a tube and then outgassed for 1 h at 110 °C prior to the measurements. The specific surface area was calculated by the Brunauer–Emmett–Teller (BET) method in the P/P° range of 0.05–0.30. Pore size distribution was determined by the Barrett–Joyner–Halenda (BJH) method based on the desorption branch of the isotherm. As a result of peak noise observed in the raw data, a three-point moving average was applied to smooth the fluctuations. Transmission electron microscopy (TEM) images were acquired using a JEOL JEM-1400 Plus microscope operated at an accelerating voltage of 120 kV.

2. Catalyst preparation and reaction procedures

Preparation procedure of SnO-XXX and MgO-XXX catalysts

SnO-XXX and MgO-XXX catalysts were prepared by calcining SnO and MgO at XXX °C for 1 h under a static air atmosphere.

Typical depolymerization procedure (Fig. 1a, b)

Catalyst (0.25 g), polyethylene glycol (PEG) (3.60 g), poly(ε-caprolactone) (PCL) (0.25 g), and a Teflon-coated magnetic stir bar were added into a 50 mL Teflon vessel. The reactor was sealed in an autoclave and purged three times with argon (0.3 MPa). After the purging, the reactor was filled with argon (0.3 MPa), heated to 180 °C, stirred at 900 rpm for 3–66 h. After stirring for the specified time, the reactor was cooled down in an ice-water bath and the gases (argon) were released. After completion, a known amount of biphenyl was added to the product mixture as an internal standard, and the mixture was diluted with tetrahydrofuran and analyzed using ^{1}H NMR. The amounts of each component in the product mixture were quantified from the ratio of the integrated peak areas of biphenyl and the corresponding protons of each species. The yield of ε-caprolactone (CL) was calculated using the following equation:

$$\text{The yield of CL} = \frac{The\ amount\ of\ CL\ obtained\ after\ reaction\ (g)}{The\ amount\ of\ PCL\ loaded\ before\ reaction\ (g)} \times 100$$

Catalyst reuse experiments procedure (Fig. 1c)

After the reaction, the used catalyst was separated from the reaction mixture by centrifugation. The obtained precipitate was washed with tetrahydrofuran and acetone in air, and then dried at 110 °C for over 3 h. The dried powder was then reused in a subsequent reaction.

Reactive distillation depolymerization procedure (Fig. 1d, e)

Catalyst (0.25 g), PEG (3.6 g), PCL (0.25 or 5.0 g), and a Teflon-coated magnetic stir bar were added into a 30 mL eggplant flask. The flask was connected in sequence to a distilling head, a Liebig condenser, and a pear-shaped receiver flask with two necks. The second neck was connected to a vacuum line via a Dimroth condenser.

The system pressure was adjusted to 20 torr, The reaction flask was heated in an oil bath at 80 °C for 30 min to melt PCL and remove residual moisture. Subsequently, the receiver flask was cooled to −15 °C to minimize loss of volatile products, and the reaction flask was then heated to 180 °C. After stirring for specified time, the reactor was cooled down in air. The distilled fraction and the residue were each quantified for their components following “the typical depolymerization procedure”. It should be noted that each fraction was diluted with chloroform instead of THF to obtain clearer ^{1}H NMR spectra.

3. Representative ^{1}H NMR spectrum of the reaction mixture

The ^{1}H NMR spectra of the residue and the distillate obtained after depolymerization of PCL under the conditions used in Fig. 1d and 1e are shown below. As shown in (i) and (iii), no signals attributable to PCL are observed; only peaks corresponding to PEG are detected. As illustrated in (ii) and (iv), CL is the predominant component in the distillate, although minor amounts of low-boiling constituents originating from the polyethylene glycol solvent (e.g., ethylene glycol and diethylene glycol) are also present. As the amount of PCL charged relative to PEG increases, these impurity signals become less pronounced.

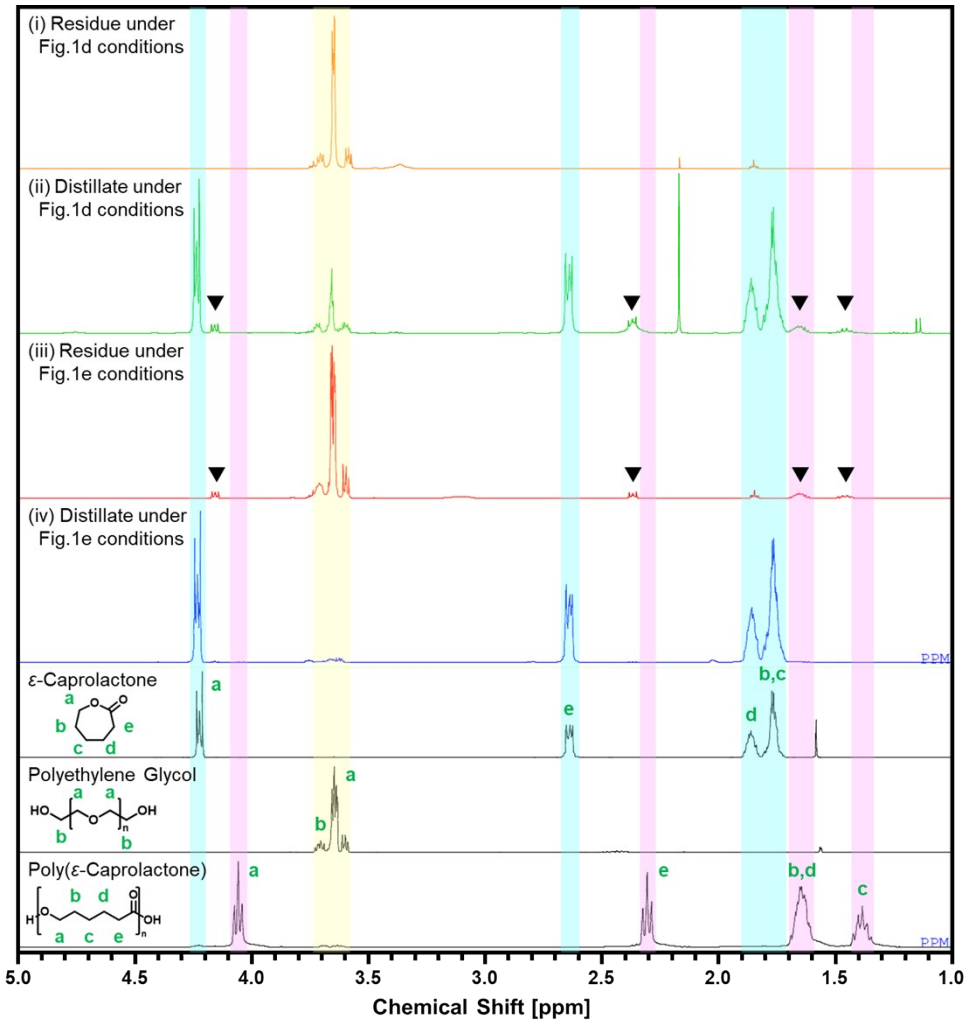

Figure S1. ^{1}H NMR spectra of the bottom residue and the distillate obtained after reactive distillation. (i), (ii): under the conditions used in Fig. 1d (PCL: 0.25 g, 16 h), (iii), (iv) under the conditions used in Fig. 1e (PCL: 5 g; reaction time: 24 h). All other reaction conditions were identical: SnO-500 (0.25 g), PEG (Mw = 400 g mol^{-1}, 3.6 g), 180 °C, under vacuum. Peaks marked with ▼ are attributed to the caprolactone dimer.

4. Quantitative analysis using ^{1}H NMR

The ^{1}H NMR spectra of the residue obtained after gram-scale depolymerization of PCL under the conditions used in Fig. 1e is shown below. As the amount of PEG relative to the charged PCL decreases, the amount of impurities relative to the resulting CL also decreased, leading to higher purity of CL. The quantification of CL was performed based on the integrated peak area ratio between the proton at position "a" of biphenyl (4H), which was added as an internal standard, and the proton at position "a" of CL (2H). In this experiment, 0.10 g of biphenyl was added, and the integrated peak area ratio in ^{1}H NMR spectra was determined to be 28.1. Based on this value, the amount of CL produced was calculated to be 4.14 g, corresponding to an 83% yield relative to the initial 5 g of PCL.

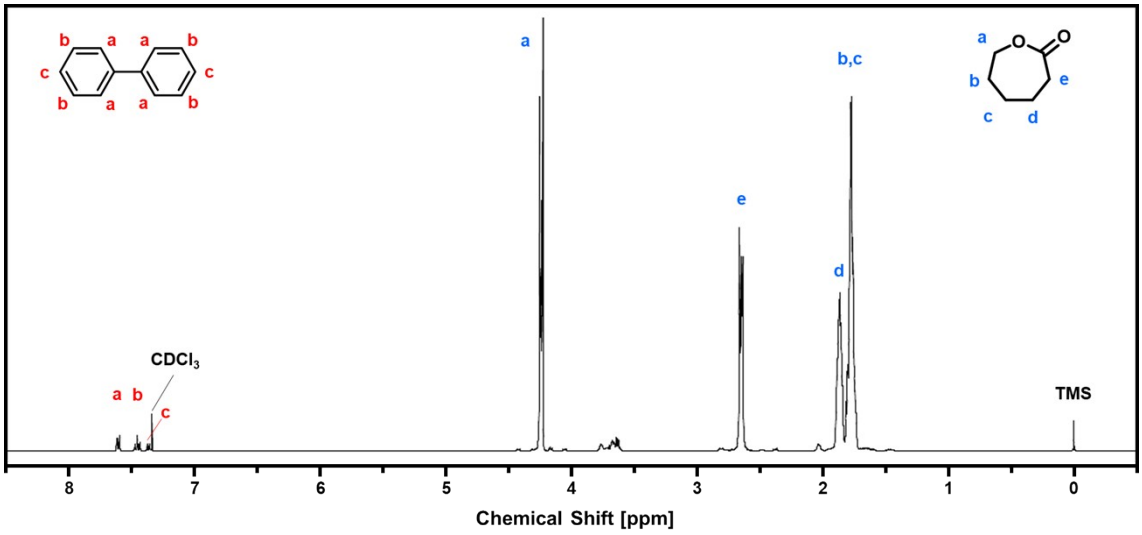

Figure S2. ^{1}H NMR spectra of the distillate obtained after gram-scale reactive distillation under the conditions used in Fig. 1e.

5. Catalytic activity of reported catalysts

Table S1. Reported catalysts for RCDP of PCL.

Catalyst[a]	Additives[b]	Reaction Conditions[c]	Reaction type	Yield	Ref.
$Bu_2Sn(OMe)_2$		PCL *M*n = 20.0 kg mol^{-1} Cat.: 0.1 mol%, 260 ºC, 1 Pa, 90 min	Reactive distillation	82%	[S2]
NaOH		PCL *M*n = 20.0 kg mol^{-1} Cat.: 0.1 mol%, 260 ºC, 1 Pa, 50 min	Reactive distillation	87%	[S2]
$Mg(HMDS)_2$		PCL *M*n = 2.0 kg mol^{-1}, Cat.: 0.1 mol%, 210 ºC, 7 Pa, 1.5 h	Reactive distillation	92%	[S3]
$ZnCl_2$	PEG600 (20 wt.%)	PCL *M*n = 64.5 kg mol^{-1}, Cat: 8 mol%, 160 ºC, 13 Pa, 16 h	Reactive distillation	96%	[S4]
$Sn(Oct)_2$		PCL *M*n = 49.7 kg mol^{-1}, Cat.: 0.05 mol%, 270 ºC, 10-20 kPa, 4.5 h	Reactive distillation	87%	[S5]
$ZnCl_2$	LLDPE (1.5 times for the initial PCL charge)	PCL *M*n = 10.0 kg mol^{-1}, Cat.: 0.05 mol%, at initial charge, 240 ºC, 85 kPa, 4.5 h	Reactive melt-blending under vacuum	80%	[S6]
BisSalen-Al complex		PCL *M*n = 35.2 kg mol^{-1}, PCL: 50mM, Cat.: 2.5 mM in Acetonitrile, 160 ºC, 0.86MPa, 18 h	Sealed reaction above solvent boiling point	93%	[S7]

[a] $Bu_2Sn(OMe)_2$: Dibutyl Tin(IV) Dimethoxide, $Mg(HMDS)_2$: Magnesium bis(hexamethyldisilazide) , $Sn(Oct)_2$: Tin(II) 2-ethylhexanoate. [b] PEG600: Polyethylene glycol (*M*w = 600 g mol^{-1}), LLDPE: linear low-density polyethylene, additive amount based on the weight ratio to PCL. [c] Catalyst loading based on the molar ratio to monomer units in PCL.

6. Detailed Comparison of Catalytic Activities among Metal Oxide Catalysts

Table S2. Comparison of catalytic performance of various metal oxides for PCL depolymerization with PEG under non-vacuum conditions. Reaction conditions: catalysts (0.25 g), PCL (0.25 g), PEG (3.6 g), Ar (0.3 MPa), 180 °C, 16 h.

Catalyst	for Bulk Weight		for Bulk Metal Amount*			for Surface Metal Amount**			
	Weight [g]	PEG-CL Yield [%]	Metal Amount [mmol]	Turnover Number	Turnover Frequency [h^{-1}]	Surface Area [m^2 g]	Metal Amount [mmol]	Turnover Number	Turnover Frequency [h^{-1}]
SnO	0.25	**12**	1.9	**0.142**	**0.009**	0.6	0.002	**133.2**	**8.33**
MgO	0.25	**16**	6.2	**0.057**	**0.004**	19.3	0.129	**2.7**	**0.17**
ZnO	0.25	**8**	3.1	**0.057**	**0.004**	4.0	0.021	**8.5**	**0.53**
TiO_2	0.25	**6**	3.1	**0.042**	**0.003**	109.5	0.435	**0.3**	**0.02**
Al_2O_3	0.25	**5**	4.9	**0.022**	**0.001**	116.9	0.685	**0.2**	**0.01**
SnO_2	0.25	**3**	1.7	**0.040**	**0.002**	5.5	0.019	**3.5**	**0.22**

* Assuming metals are present at concentrations according to the stoichiometric formula.

** Assuming metals are uniformly dispersed, with those within the outermost 0.3 nm exposed at the surface.

7. Time course of depolymerization

Depolymerization of PCL over SnO-500 catalyst was performed for various reaction times to monitor the time-dependent yield of PEG-CL. The PEG-CL yield plateaued after 24 h, indicating that the reaction reached equilibrium.

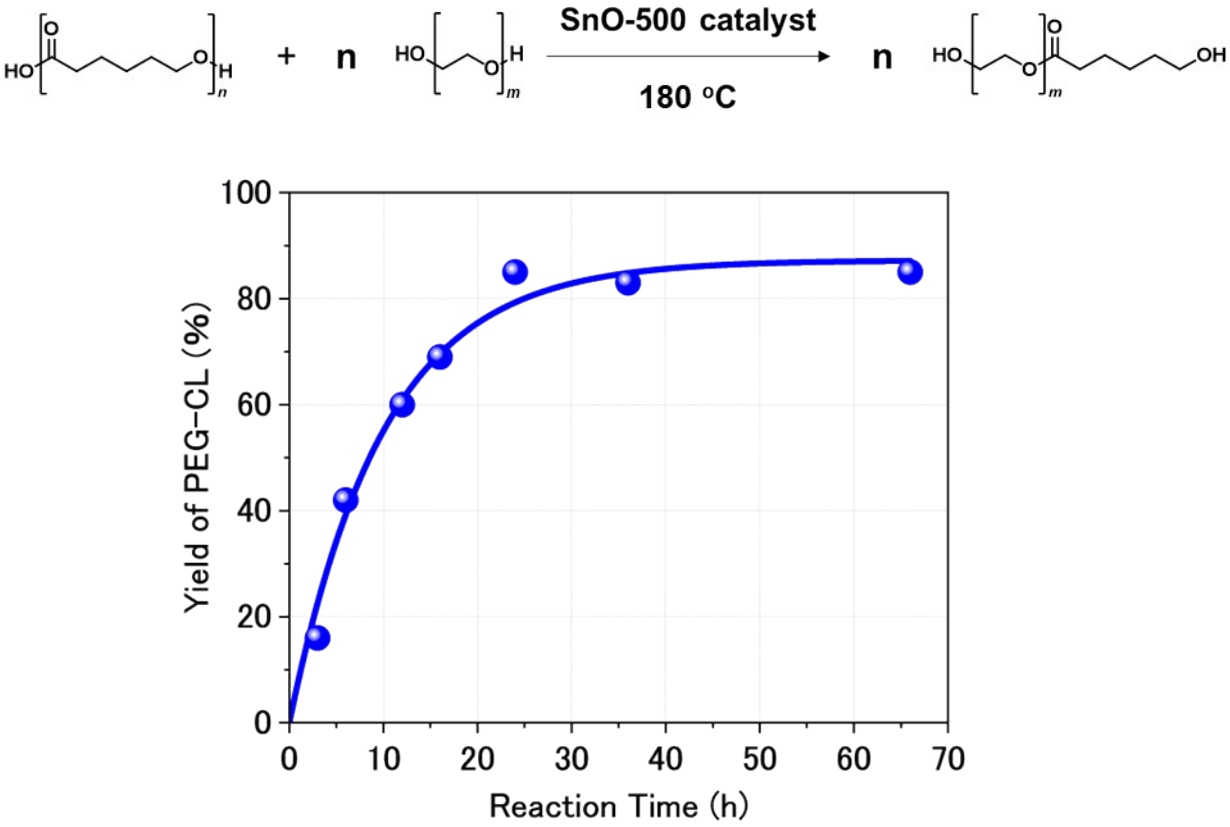

Figure S3. Time-dependent change in PEG-CL yield during PCL depolymerization over SnO-500 catalyst. Reaction conditions: SnO-500 (0.25 g), PCL (0.25 g), PEG (3.60 g), Ar (0.3 MPa), 180 °C.

8. Hot filtration test using the SnO-500 catalyst

After a 6-hour typical depolymerization using the SnO-500 catalyst, the mixture was subjected to hot filtration to remove the catalyst while maintaining the solution temperature. The filtrate was further heated for an additional 10 h, after which the PEG-CL content in the reaction mixture was analyzed by ^{1}H NMR spectroscopy. As a result, no further progress of the reaction was observed after 6 h, indicating that the reaction occurs on the solid surface.

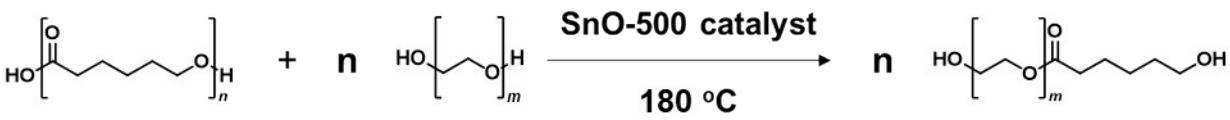

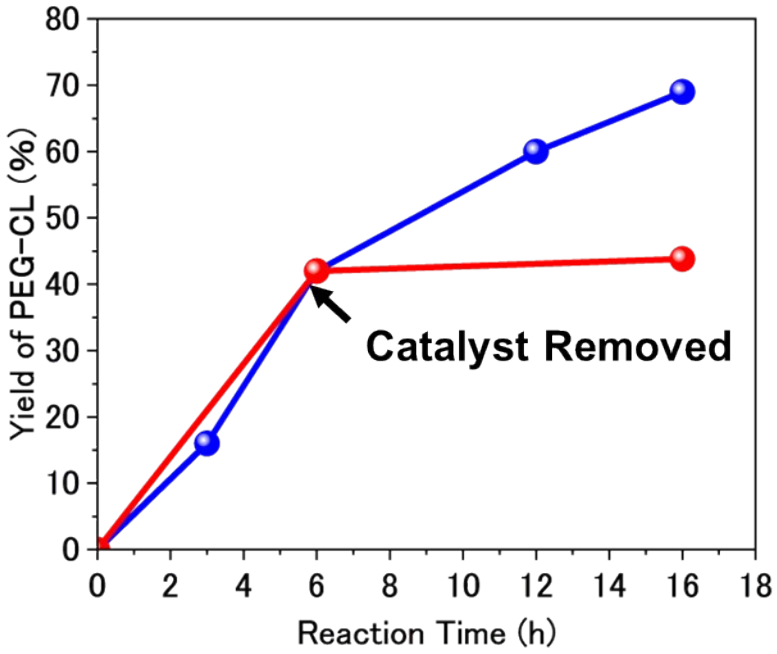

Figure S4. Hot filtration experiment of the SnO-500 catalyst: (blue line) without filtration of the catalyst and (red line) with removal of the catalyst by hot filtration after 6 h. Reaction conditions: SnO-500 (initial: 0.25 g), PCL (0.25 g), PEG (3.60 g), Ar (0.3 MPa), 180 °C.

9. Detailed structural change analysis using in-situ SXRD

Structural changes of SnO during heating from 300 °C to 550 °C were investigated by in-situ SXRD. In this graph, the point at which each trace intersects the vertical axis represents the measurement temperature. The peak corresponding to the SnO_2 (101) plane at $2\theta = 6.1°$ appears between 400 °C and 500 °C, and becomes clearly visible above 500°C. This is consistent with disproportionation occurring between 400 °C and 500 °C, resulting in an increase in pore volume and specific surface area.

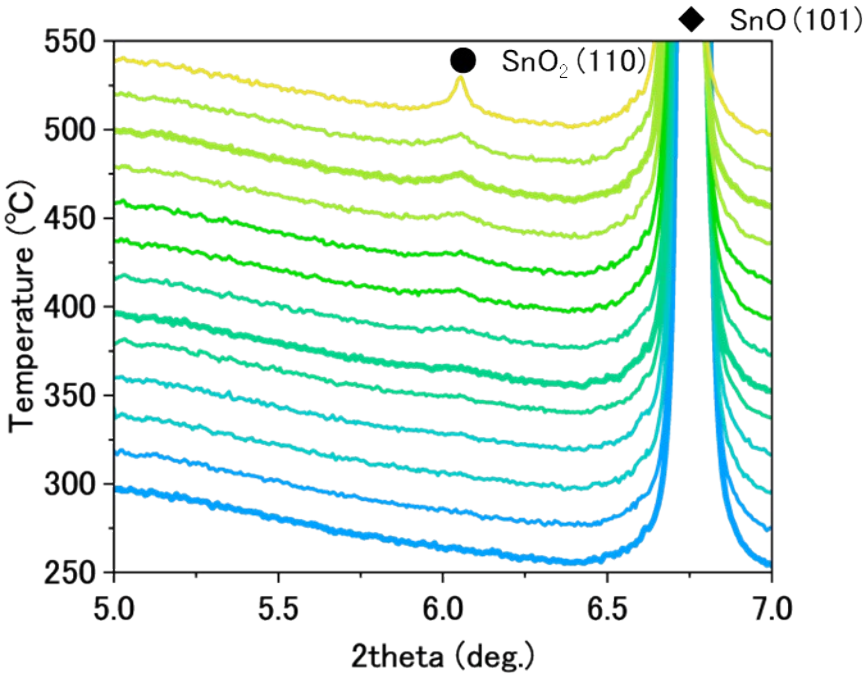

Figure S5. SXRD patterns for SnO collected at 20 °C intervals measured continuously during heating from 300 °C to 550 °C in air at a rate of 80 °C min^{-1}, using synchrotron radiation (λ = 0.354443 Å). The measurement temperature for each SXRD pattern is indicated by its intersection with the vertical axis.

10. Structural analysis of SnO after heat treatment

After calcination at 500 °C in air, diffraction peaks of metallic Sn were observed, although they were not seen during in-situ SXRD. Since Sn melts at 232 °C,[S8] it likely existed in liquid form during heating and crystallized upon cooling. Metallic Sn was not found after calcination at 300 °C, but appeared at 400 °C, suggesting that disproportionation starts at around this temperature. In the in-situ SXRD experiment, the heating rate was 80 °C min^{-1}, so the onset temperature may be slightly higher. The coexistence of Sn and SnO_2 after calcination at 500 °C under N_2 atmosphere indicates that SnO_2 forms through disproportionation rather than simple oxidation. Peaks approximately 27° and 32° in samples treated at 500 °C in air and N_2 are attributed to Sn_2O_3, a possible intermediate phase during the transformation of SnO to SnO_2.[S9,S10]

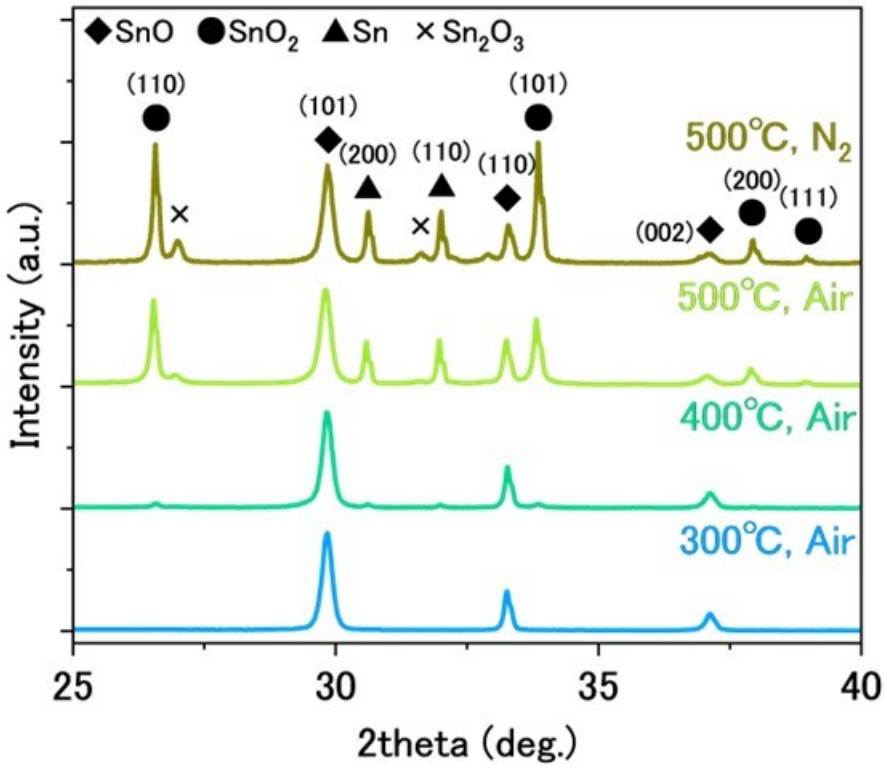

Figure S6. Ex-situ XRD patterns of SnO after calcination.

11. Morphological Transformation of SnO During Calcination at 500 °C

The morphology of SnO before and after calcination at 500 °C was observed by TEM. Before calcination, large (>100 nm) particles without visible grain boundaries are observed (a, b), whereas after calcination, sub-100 nm particles with distinct grain boundaries are clearly aggregated (c). The crystallite size calculated from XRD remained approximately 50 nm before and after calcination, indicating that the size of the primary particles did not change. This suggests that the dense polycrystalline structure broke apart into individual particles during heating, creating more gaps between them. Additionally, some plate-like stacked structures were also observed after calcination (d).

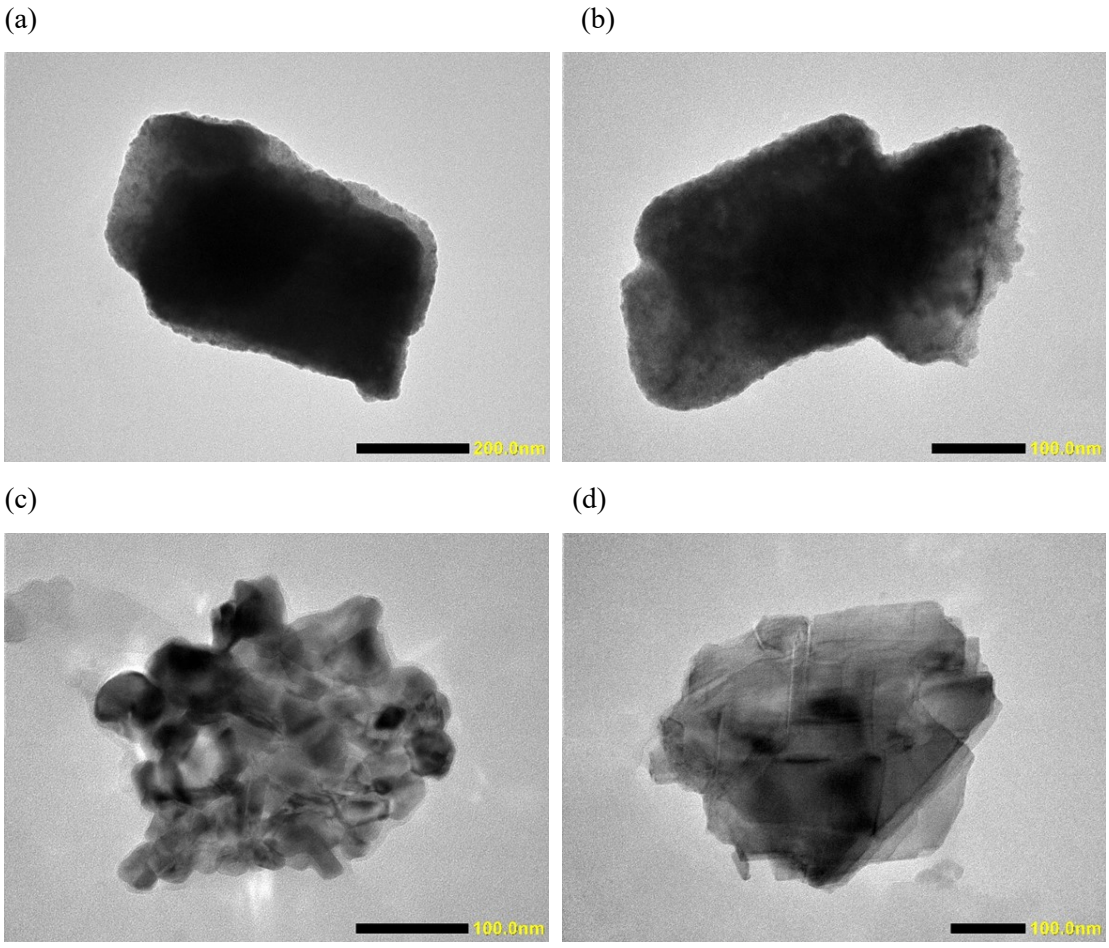

Figure S7. TEM images of SnO (a), (b) before and (c), (d) after calcination at 500 °C for 1 h.

12. Supplementary Reference

S1. S. Kawaguchi, S. Kobayashi, H. Yamada, H. Ashitani, M. Takemoto, Y. Imai, T. Hatsui, K. Sugimoto and O. Sakata, *J. Synchrotron Radiat.*, 2024, **31**, 955–967.

S2. M. Nelißen, H. Keul and H. Höcker, *Macromol. Chem. Phys.*, 1995, **196**, 1645–1661.

S3. J. Sun, G. Xu, B. Du, R. Yu, H. Sun and Q. Wang, *Polym. Chem.*, 2022, **13**, 5897–5904.

S4. C. F. Gallin, W.-W. Lee and J. A. Byers, *Angew. Chem. Int. Ed.*, 2023, **62**, e202303762.

S5. C. Cai, J. Ma, X. Liang, S. Zhang, H. Zhang, C. Zhang and S. Zhang, *Polym. Chem.*, 2025, **16**, 1568–1577.

S6. A. Sarmah, A. J. Zervoudakis, M. R. Pfau-Cloud, M. A. Hillmyer and C. J. Ellison, *ACS Appl. Polym. Mater.*, 2025, **7**, 1763–1770.

S7. R. Yang, W. Wei, G. Xu, X. Guo and Q. Wang, *Angew. Chem. Int. Ed.*, 2025, **64**, e202504819.

S8. Y. Zhang, J. Liu, X. Wang, Y. Li, Y. Zhao and H. Zhang, *J. Mater. Sci.: Mater. Electron.*, 2024, **35**, 4567–4579.

S9. W. K. Choi, H. Sung, K. H. Kim, J. S. Cho, S. C. Choi, H.-J. Jung, S. K. Koh, C. M. Lee and K. Jeong, *J. Mater. Sci. Lett.*, 1997, **16**, 1551–1554.

S10. J.-H. Zhao, R.-Q. Tan, Y. Yang, W. Xu, J. Li, W.-F. Shen, G.-Q. Wu, X.-F. Yang and W.-J. Song, *Chin. Phys. B*, 2015, **24**, 070505.